Accepted Manuscript

Temperature dependent ultrasonic and thermo-physical properties of polyaniline nanofibers reinforced epoxy composites

Meher Wan, R.R. Yadav, Devraj Singh, M. Sridhar Panday, V. Rajendran

PII: S1359-8368(15)00629-0

DOI: 10.1016/j.compositesb.2015.10.011

Reference: JCOMB 3842

To appear in: *Composites Part B*

Received Date: 7 April 2015

Revised Date: 30 August 2015

Accepted Date: 20 October 2015

Please cite this article as: Wan M, Yadav RR, Singh D, Sridhar Panday M, Rajendran V, Temperature dependent ultrasonic and thermo-physical properties of polyaniline nanofibers reinforced epoxy composites, *Composites Part B* (2015), doi: 10.1016/j.compositesb.2015.10.011.

This is a PDF file of an unedited manuscript that has been accepted for publication. As a service to our customers we are providing this early version of the manuscript. The manuscript will undergo copyediting, typesetting, and review of the resulting proof before it is published in its final form. Please note that during the production process errors may be discovered which could affect the content, and all legal disclaimers that apply to the journal pertain.

ACCEPTED MANUSCRIPT

Temperature dependent ultrasonic and thermo-physical properties of polyaniline nanofibers reinforced epoxy composites

Meher Wan[1, 4*], R.R.Yadav[1], Devraj Singh[2], M Sridhar Panday[3], V.Rajendran[3]

[1]*Physics Department, University of Allahabad, Allahabad-211002, India*

[2]*Department of Applied Physics, Amity School of Engineering and Technology, Bijwasan, New Delhi-110061, India*

[3]*Centre for Nano Science & Technology, K.S. Rangasamy College of Technology, Tiruchengode, India*

[4]*Department of Metallurgical and Materials Engineering, Indian Institute of Technology, Kharagpur-721302, India*

[*]Email- meherwan24@hotmail.com
Tel. / Fax: +91 532 2460987/ +91 532 2460993

Abstract

Epoxy based all polymer nanocomposites reinforced with Polyaniline (PANI) nanofibers have been prepared via sono-chemical route. Ultrasonic velocity, attenuation and thermal conductivity are measured in a wide temperature range (298-373 K) at different PANI nanofibers loadings (1 & 2 wt %) in PANI-Epoxy nanocomposites. Behavior of thermal conductivity and ultrasonic attenuation with temperature in synthesized nanocomposites is explained with help of existing phenomena. Increase in ultrasonic velocity and thus longitudinal modulus with reinforcement of nanofibers indicates that strong cohesive interaction force, which rises among the nanofibers and matrix elements.

Key words: A. Nanostructures; A. Polymer-matrix Composites; D. Ultrasonics; B. Thermal Properties; B. Mechanical Properties.

1. Introduction

The applications of epoxy nanocomposites are being incresed very rapidly in our daily life.[1] Despite having high tensile strength, Young's modulus and electrical insulating properties [2, 3] with its potentially wide applications in adhesives, [4] electronics (excellent electrical insulators),[5] mechanical properties [6, 7] for marine and aerospace industry etc. [8, 9] epoxy is very conventional and easy to synthesize engineering thermosetting polymer. Three dimensional nanowire networks are attacting the attenion of researchers due to their nano-structure based advanced physical and chemical properties.[10, 11] Combining Polyaniline (PANI) with epoxy resin is a good strategy to obtain thermosetting composites having better dielectric properties. Electrically conductive composites are promising materials for various applications such as electromagnetic shielding [12], antistatic applications [13] and conductive adhesives [14]. Due to their excellent mechanical and electrical properties nanocomposites of PANI, with polymer matrices such as epoxy, have potential applications in modern technologies such as microwave absorption, electromagnetic shielding, sensor materials and conducting glues [15]. *De facto*, interfacial compatibility and bonding between polymer matrix and filler nanostructures are very important parameters to maintain the mechanical properties of composites and isotropy. Various surfactant and polymers are very useful in order to enhance interfacial matrix-filler interaction [16] for metal oxide nanoparticles as fillers. As a coupling agent, Polyaniline is very useful to enhance the dispersability and interfacial interaction. Due to the presence of unique -amine and '-imine' groups in its backbone [17], it is a useful functionalizing agent [18 and references their-in].

Ultrasonics is one of the non-destructive characterization techniques, which provides the insight for different properties of a wide range of materials without destrying the materials. Elastic modulii can be calculated from the ultrasonic velocity data in longitudinal and shear mode for crystalline materials.[19] The theory for the calculation of elastic modulii and ultrasonic attenuation in crystalline materials is well known and established.[20] Ultrasonic attenuation is also well related with the thermal conduction in crystalline materials.[19] The development of composite materials with nano-structured filler materials opened a space for research regarding ultrasonic properties. Due to great importance of

polymer nanocomposites in industrial world, the analysis of different properties via ultrasonic parameters is worth study.

In the present research work, we have fabricated the PANI nanofibers reinforced in epoxy nanocomposites following the definite chemical route with the help of mild ultrasonic waves. Micro-structural characterization and study of Fourier transform infrared spectroscopy (FTIR) has been done for the samples. Experimental study of ultrasonic properties has been used to extract the information about the structure and different thermo-physical properties. Experimental study of temperature/concentration dependent thermal conductivity has also been done leading to different industrial applications.

2. Experimental

2.1 Synthesis of Nanocomposites

Epoxy LY 556 resin (Bisphenol-A-Diglycidyl-Ether) was employed as matrix resin. The epoxy resin (Araldite LY 556) and the corresponding hardener (HY 951) were mixed in a recommended ratio. The filler nanostructures of Polyaniline were synthesized with the oxidative polymerization of aniline monomer in which Potassium Biiodate was used as oxidant at ambient conditions. The detailed mechanism of polymerization of aniline monomer in to polyaniline is mentioned in our previous research work [20].

The Epoxy resin and Polyaniline nanofibers were dispersed in acetone in different weight ratios of 1 and 2 wt% and further the mixtures were ultrasonicated for uniform dispersion of fillers in the base matrix. After sonication, the hardener was added to the suspensions and the samples were again ultrasonicated with 100Watt intensity at 20 kHz ultrasonic frequency (Sonics VC 505). Then, the solvent, acetone was evaporated at 60^0C for 5 hours. Samples of pure epoxy and composites of 1 and 2 wt% PANI-epoxy were cured at 120 ^{0}C for 6 hours.

2.2 Structural and Morphological Characterization

The surface morphology analysis of the samples was conducted by a scanning electron microscope (Zeiss EVO MA-10 SEM operating at 5.0 keV). The dried powder product of Polyaniline was coated on the carbon tape for SEM characterization. From SEM photographs [Fig. 1 (a, b, c & d)], it is confirmed that the product is fibril in structure and embedded well in epoxy matrix. Fibril structures of Polyaniline (PANI) have average diameters of 50 nm; and the average length of nanofibers is more than one micrometer. Fig.

1(a) is SEM photograph clean epoxy; Fig.1 (b) is for Polyaniline nanofibers and Fig. (c & d) are the photographs of 1 & 2 wt&% PANI-epoxy nanocomposites. FTIR spectroscopy is used to observe the changes in the structure of epoxy matrix due to Polyaniline nanofibers. Fig. 2 shows the FTIR spectra of pure epoxy and 1 &2 wt% Polyaniline-epoxy nanocomposites. It can be easily observed that characteristic peaks corresponding to Polyaniline are emerged in spectra of nanocomposites. The peaks at 1246 and 1300 cm^{-1} were attributed to C–H stretching from aromatic conjugation which corresponds to characteristic peaks of Polyaniline. Peaks at 1483 and 1567 cm^{-1} also correspond to Polyaniline nanostructures, which also were emerged in the spectra of epoxy after mixing of Polyaniline.

2.3 Ultrasonic, thermal characterization

For ultrasonic measurements a high-power ultrasonic pulser receiver (5900 PR; Olympus NDT, USA) and a digital storage oscilloscope (DSO; Wave Runner 104 MXi 1GHz; Lecroy) is used for recording ultrasonic signals at a frequency of 5 MHz. In the present experimental set-up, one can obtain the required temperature by either dynamic mode or static mode depending on the requirements, using Eurotherm temperature controller. The accuracy of the temperature in the sample region was ±1 K. To provide proper impedance matching, a good contact was established between the sample, the waveguides and the transducers. Further the opposite surfaces of both the sample and the waveguides were polished properly for the propagation of the ultrasonic waves into the sample. Ultrasonic velocity and attenuation measurements were performed through conventional transmission technique. The details of ultrasonic velocity in samples is calculated with the transit time of ultrasonic wave and sample thickness with formula given below-

$$U = \frac{d}{\Delta t} \tag{1}$$

If the sample thickness (d) is known in micron resolution and transit time ($\triangle t$) in nanosecond resolution, the overall accuracy obtained in the measurement of velocity was ±2 m s^{-1}. The attenuation of the ultrasonic waves in the sample was determined using the relation [21]:

$$\alpha(f) = \frac{1}{d}\left(1nT + 1n\left(\frac{A_w(f)}{A_s(f)}\right)\right) \tag{2}$$

Where, $A_w(f)$ is the amplitude of the received signal with the waveguides only and $A_s(f)$ refers to the amplitude of the received signal with sample inserted between the waveguides. The transmission coefficient (T) at the interface of the sample and the waveguide was obtained using the relation:

$$T = \frac{4 Z_w Z_s}{(Z_w + Z_s)^2} \quad (3)$$

Where, Z_w and Z_s respectively are the acoustic impedances of the waveguide and the sample. The couplant correction for the measured velocity and attenuation was carried out by the standard procedure.[21]

Thermal conductivity of nanofluids was measured using the Hot Disk Thermal Constants Analyzer (Hot Disk Inc., Uppsala, Sweden). The apparatus uses the transient plane source (TPS) method for measuring the thermal conductivities of nanocomplosites/fluids. Details of instrumentation is given in our previous work.[20] The uncertainties of the TPS method are about 2%. TPS method is modified version of Transient Hot Wire technique for heat transfer measurements.

3. Result and discussion

3.1 Ultrasonic Characterization of PANI-Epoxy Nanocomposites

The fiber-matrix inter-phase plays an important role in determining composite performance. The inter-phase/bonding between filler and matrix affects the mechanical properties by allowing the load transfer between filler nanostructures and matrix; and provides a platform for chemical and thermal compatibility between the constituents.[22] The ultrasonic velocity is increasing in the composites with the filler concentration in the base matrix [Fig. 3]. This increase in the ultrasonic velocity shows that in the samples the longitudinal modulus (B) is increasing more than the increase in density of composites due to particle loading of Polyaniline in epoxy as it is clear by the following formulations. Ultrasonic velocity is given as:

$$V = \sqrt{B / \rho_{eff}} = 1/\sqrt{k\,\rho_{eff}} \quad ; \mathrm{k} = \mathrm{B}^{-1} = (\lambda + 2\mu)^{-1} \quad (4)$$

where, B, ρ_{eff}, k are the Longitudinal modulus, effective density and compressibility of the medium. The symbols λ and μ are Lame moduli. Effective density and compressibility can be written as-

$$\left.\begin{aligned}\rho_{eff} &= \rho_s\phi + \rho_m(1-\phi)\\ k_{eff} &= k_s\phi + B_m^{-1}(1-\phi)\end{aligned}\right\} \quad (5)$$

Where, φ is Particle volume fraction. Subscripts *s* and *m* refer to nanofibers system and base matrix. According to above equations, the change in density and Longitudinal modulus/Lame moduli with volume fraction causes an enhancement in ultrasonic velocity. By the dispersion of nanofibers, the velocity increase indicates that after dispersion of nanofibers in epoxy matrix, a strong cohesive interaction force rises among the molecules/atoms which results a large increase in longitudinal modulus. Change in density of the composite due to nanoparticles loading is insignificant.

Decrease in ultrasonic velocity with temperature indicates that the longitudinal modulus is decreasing with the increase in temperature. The decrease in longitudinal modulus with temperature is due to the softening of the lattice structure or increase in the lattice disorder.[23] Longitudinal modulus has been calculated from the ultrasonic velocity in all compositions for the same temperature range [Fig. 4], which is comparable with the values available in the literature for epoxy matrices.[24] One of the reasons for the increase in Bulk modulus of nano-composite is that the PANI nanofibers have good interfaces with the epoxy matrix. Nanofibers make strong contacts with epoxy matrix which causes an increase in longitudinal modulus of nanocomposites in comparison to pure epoxy.

Further, ultrasonic attenuation is very important parameter for a material which gives the information about the micro-structural and thermo-physical properties of a material. The attenuation in the pure epoxy and 1 & 2 wt% PANI-epoxy nanocomposites is measured in temperature range 300-373 K with pulse echo technique [Fig. 5]. Ultrasonic attenuation decreases with particle loadings and increases with temperature on dispersion of Polyaniline nanofibers in epoxy matrix.

Ultrasonic attenuation decreases with enhancement in crystallinity of material. Polyaniline nanofibers possess better crystalline nature in comparison to epoxy matrix. Thus,

it may be stated that the reason behind the decrease in ultrasonic attenuation in nanocomposites is due to improvement in crystalline content in it with reinforcement of polyaniline nanofibers in epoxy. Thermal loss is caused by temperature variation produced by propagation of sound waves in different parts of suspension. Increase in attenuation with temperature is due to softening of bonds between the constituent atoms in the matrix.

Ultrasonic attenuation is large in amorphous materials in comparison to crystalline materials due to complicated relationship with temperature, frequency and density.[25] In the composite materials, mechanism responsible for ultrasonic attenuation is complex. It involves viscoelastic, scattering and thermal losses. The relative contribution of these losses to total attenuation may change with the particle size and concentration of reinforcing agent at a particular frequency, acoustic properties of polymer matrix and reinforced particles. Attenuation is mainly contributed to viscoelastic and scattering effects due to retardation phenomenon between strain and stress in polymeric materials. Presence of heterogeneity in the polymeric materials (i.e. multiphase and semi-crystallinity) contributes scattering factor to ultrasonic attenuation. Ultrasonic attenuation as a function of concentration of micro-scaled filler material is caused by scattering in low frequency regime was calculated by Biwa and his co-workers. The calculated dependence of ultrasonic attenuation with concentration is [25]:

$$\frac{d\alpha}{d\phi} = -\alpha + \frac{\gamma^{sca}}{(8/3)\pi r^3} \tag{6}$$

The scattering cross-section γ^{sca} depends on the particle radius *r*, the frequency of wave *f*, Longitudinal modulus or Lame moduli and density of base matrix ρ, including the morphology of nanofibers which were embedded in base matrix and particle volume fraction'φ'.

$$\gamma^{sca} = \gamma^{sca}(\lambda_{st}, \mu_{st}, \rho, \lambda_2, \mu_2, \rho_2, f, r) \tag{7}$$

Thus, the functional dependence of scattering cross section γ^{sca} is determined by the properties of host matrix static lame modulii λ_{st}, μ_{st} and the properties of reinforced particles λ_2, μ_2 and density ρ_2. The parameters λ, μ and ρ are the Lame moduli and density of the composite. The scattering cross section is influenced by particle radius to sound wavelength ratio and acoustic mismatch between particle and host matrix. Biwa *et al.* [25] computed the

attenuation in glass/epoxy composites for different volume fraction of particle loadings at various particle radius-to-wavelength ratios. The decreasing behavior of ultrasonic attenuation is found with volume fraction of particle loadings. This decreasing behavior of attenuation is result of the minor scattering loss when the scatterer dimension is much smaller than the incident sound wavelength. The viscoelastic loss contributes mainly to the total attenuation in the composite which decreases as the volume fraction of the particles increases in the host matrix of epoxy.

Effect of temperature on ultrasonic attenuation in nanocomposites can be explained with the relaxation phenomenon. Relaxation phenomenon can be observed at all ultrasonic frequencies practically which originates from the modulation of thermal equilibrium of subsystem in a sample by strain and stress field of the mechanical wave. Due to propagation of ultrasonic wave in a medium, the perturbed subsystem tries to relax in the new equilibrium by exchanging energy. In this process, the entropy is increased due to delayed response of the relaxing system and thus wave is attenuated. It was found in experiments for the case of vitreous silica [26] that the relaxation time τ has Arrhenius equation type of relationship with temperature, which can be written as-

$$\tau = \tau_0 \exp\left(\frac{-E_a}{K_B T}\right) \tag{8}$$

Where, τ_0 is a constant of the order of 10^{-13} second for vitreous silica and E_0 is the activation energy for relaxation process. The same behavior of ultrasonic attenuation is observed with temperature in our case of Polyaniline/epoxy nanocomposites. Thus, the increase of ultrasonic attenuation is justified with the temperature with relaxation mechanism.

3.2 Thermal Characterization of PANI-Epoxy Nanocomposites

Thermal conductivity of amorphous solids is much less in comparison to crystalline materials. It shows the decreasing behavior with temperature monotonically which is almost independent of chemical composition of amorphous materials. The heat conduction in polymers is performed mainly by phonons. The scattering of phonons must have a very common and simple origin in amorphous solids which is extremely independent of structural details or vibrational spectrum of these solids. Unlike pure crystalline solids, where the lattice defects in the form of impurities cause the local changes in these vibrations are referred as

defect modes and depend upon types and concentration of defects,[27] in amorphous solids, a different kind of defect mode has been observed which leads to characteristic changes in thermal conductivity at different temperatures. According to Han *et al.* [28] thermal conductivity of polymers ranges from ~0.20 to 0.70 W/mK due to large scattering of phonons. They illustrated that thermal conductivity is greatly affected by the level of crystallinity in the polymers; it varies almost linearly with the crystallinity. Thermal conductivity of polymers also depends on the several other factors like chemical constituents, bond length, structure type, side group molecular weight, molecular density distribution, type and strength of structural faults, processing conditions and temperature. Thermal conductivity of amorphous materials increases with temperature up to glass transition temperature (T_g) and shows decreasing behavior above it. In epoxy resin, which is partially crystalline polymer, thermal conductivity increases in common temperature range (298-373K) and this order of conductivity is slightly higher in crystalline regions in comparison to amorphous regions.[29]

Thermal conductivity measurements were done on the samples of pure epoxy and 1 & 2 wt % PANI-epoxy nanocomposites in a wide temperature range (298 to 373 K) [Fig. 6]. Thermal conductivity is measured with Hot Disk Thermal Constants Analyzer (TPS 500) which is based on transient plane source method. A perusal of Fig. 6 reveals that the thermal conductivity is showing the increasing behavior with temperature. With particles loading in epoxy matrix, thermal conductivity has been increased in the dielectric matrix of epoxy polymer. This can be explained with the phonon assisted fraction hopping which predicts the linear temperature dependence of thermal conductivity[30], which is widely cited for amorphous solids. The ratio of change in thermal conductivity with temperature (dK/dT) starts decreasing at higher temperatures after 500K in amorphous solids.[31]

The obtained experimental results can be explained with the effective medium theory (EMT). Effective medium theory is used to explain the effective micro-structural properties of micro-structurally heterogeneous materials. Assuming a homogeneous and isotropic effective medium with property k_0 and a perturbation in property $k'(r)$, due to the presence of the filler, the property of the heterogeneous medium at position r is thus expressed as: $k(r) = k_0 + k'(r)$. Maxwell-Garnett approximation is based on effective medium approach, which is known to produce reasonable compatibility with experimental results for the some polymer matrices based composites with small particle loadings. The Maxwell-Garnett model does not account the shape and morphology of filler material thus can't correctly predict the thermal

conductivity for various particle loadings of different particles sizes and materials.[32] An alternative approach is the percolation mechanism, which assumes that the conduction in composites happens through the chains formed by the nanofibers/rods in the base matrix. Interfacial resistance at the contact points of these nano-structures play very important role in heat transfer mechanism. Including interface thermal resistance i.e. Kapitza resistance R_i, Nan *et al.* [33] derived the given formula for effective thermal conductivity –

$$K = K_m + \frac{K_f L}{2R_i K_f + L}\langle \cos^2\theta \rangle V_f \tag{9}$$

Where, K, K_m and K_f are thermal conductivities of composite, matrix and filler material respectively. Also, the symbols L, θ, V_f and R_i (~10^{-8} $m^2K^{-1}W^{-1}$) represent the length of filler fibres, mutual orientation of fibres, particle volume fraction and interfacial resistance respectively. Again, this formula does not account the nano-dimensionality of the filler nanostructures, thus literature shows that this model predicts lower effective thermal conductivity than reported for nanocomposites. A formulation of effective medium theory incorporating interfacial resistance approach for nano-fibre like filler structures in polymer matrix gives good correlation with experimental results for effective thermal conductivity of nanocomposites, in which nano-fibres/rods are randomly distributed in host medium i.e. base matrix. The equation for effective thermal conductivity can be written as-

$$K = K_m \frac{\left(3 + V_f\left(\beta_1 + \beta_2\right)\right)}{3 - V_f \beta_1} \tag{10}$$

Where,

$$\beta_1 = \frac{2\left\{d(K_f - K_m) - 2R_i K_f K_m\right\}}{d(K_f + K_m) + 2R_i K_f K_m} \tag{11a}$$

$$\beta_2 = \frac{L(K_f - K_m) - 2R_i K_f K_m}{LK_m + 2R_i K_f K_m} \tag{11b}$$

The symbols *d* and *L* represent the diameter and length of nanofibers in above equations, rest symbols are same as defined in above equations [35, 36]. Since, phonons play an important role in heat conduction process in electrically insulating materials, thus phonon-phonon scattering and phonon-defects scattering mechanism (grain boundaries, lattice defects

and crystallinity of filler material) control the conduction process. At room temperature, average mean free phonon path is approximately equal to inter-scattering centres in nanocomposites, which vary with the temperature of the material. To analyse the effect of temperature on thermal conductivity a sets of data points can be analyzed from an activation energy perspective. According to Balakrishnan *et al.*, [37] an Arrhenius type equation can be used for this purpose which can be written as-

$$K(T) = K_0 \exp\left(\frac{-E_a}{K_B T}\right) \tag{12}$$

Where, K is the effective conductivity in W/mK, K_B is the Boltzmann's constant in J/mol. KB = 8.31 J/(mol K), E_a is the activation energy in J/(mol). A straight line fit is obtained for the data points for plots between 1/T and ln(K). K_0 is the intercept of the straight line fit in the plot. Thus, the thermal conductivity K(W/mK) can be fitted as a function of the absolute temperature T(K) to following equation:

$$K(T) = K(T_0)\left\{F_0 + F_1\left(\frac{T}{T_0}\right)\right\} \tag{13}$$

Where, the $K(T_0)$ is the thermal conductivity at room temperature T_0 (298.15 K). F_0 and F_1 are constants can be calculated by experimental data using least square method [38]. The polymer/particle i.e. filler/matrix interfacial area is maximized by the large surface to volume ratios of the nanoparticles in a polymer nanocomposites. In the case of percolating networks, for small particle size, the number of contact points between nanofibers increase thus higher the thermal conduction in composites. With these reasons, it can be concluded that the interfaces significantly affects the thermal conductivity of nanocomposites.

The thermal conductivity and ultrasonic attenuation are directly correlated parameters as both parameters measure the damping of elastic waves in the materials. Thermal conductivity have the dependence on ultrasonic attenuation $\alpha(\omega, T)$ according to kinetic formula-

$$K(T) = \frac{1}{3}\int d\omega C(\omega, T)\Lambda(\omega, T)v \tag{14}$$

Where, $C(\omega,T)$ is the specific heat per unit volume contribution of phonons with angular frequency'ω'. $\Lambda(\omega,T)$ is mean free path of these phonons which is inversely

proportional to ultrasonic attenuation α(ω, T) and v is velocity of phonons. According to above equation, both longitudinal and transverse phonons contribute in the conduction of heat. The transverse phonons contribute more in specific heat in comparison to longitudinal modes of phonons. Still, the possibility exists that longitudinal phonons may contribute in thermal conduction with large Λ(ω,T), this contribution is larger than expected from considerations of density of states only. Since, precise contribution of phonons having longitudinal and transverse polarizations is not possible to measure, average mean free path of phonons can be considered for the explaining the thermal conduction behavior. At particular temperature, the process of heat conduction is predominantly performed by the waves which contribute the most to specific heat. Mean free path of phonon in filler nanofibers can be calculated directly by measuring the ultrasonic attenuation (as Λ is inversely proportional to α) in a solid. The relation between mean free path (*l*) of phonon and ultrasonic attenuation is [31]-

$$\frac{\lambda}{\Lambda} = \frac{v}{\omega}\alpha \tag{15}$$

Where 'ω' is the frequency and 'λ' is the wavelength of ultrasonic wave and '*v*' is Debye average velocity in the amorphous solids. This ratio of Phonon wavelength and phonon mean free path remains constant and is material independent with some exceptions. A perusal of Fig. 5 & 6 reveals the fact that the thermal conductivity is increasing with nanofibers loading and the ultrasonic attenuation is decreasing with fibres loading. Therefore on the basis of preceding theory it may be concluded that the phonon mean free path is increasing due to loading of nanoparticles with better crystallinity. When we consider the temperature dependency of thermal conductivity and ultrasonic attenuation, it is clear from the figures (5 & 6) that thermal relaxation phenomenon is dominating and consequently ultrasonic attenuation and thermal conductivity both are increasing with temperature due to increase in thermal relaxation time as in case of crystalline solids.[39]

4. Conclusions

To summarize, it is stated that the nanocomposites of Polyaniline nanofibers reinforced in epoxy are successfully synthesized with the chemical routes for different concentrations of Polyaniline nanofibers. The ultrasonic velocity, ultrasonic attenuation and thermal conductivity are measured in the wide temperature range of 298-373 K in the

samples. Ultrasonic velocity is showing decreasing behavior with the temperature and it is increasing with concentration of Polyaniline nanofibers in epoxy matrix. The behavior of phonon mean free path, ultrasonic attenuation and thermal conductivity with reference to particle loading is correlated. Polyaniline nanofibers based nanocomposites have better crystallinity in comparison to pure epoxy matrix. Temperature dependence behavior of ultrasonic attenuation and thermal conductivity gives the information about thermal relaxation phenomenon. The employed theoretical approaches for the ultrasonic attenuation and the thermal conductivity explain successfully the experimental observations.

Acknowledgements

Meher Wan is grateful to Council of Scientific and Industrial Research, New Delhi for financial support and Fellowship.

References:

[1] A. A. Azeez, K. Y. Rhee, S. J. Park, D. Hui, Epoxy clay nanocomposites – processing, properties and applications: A review, Composites Part B: Engineering, 45:1, (2013) 308–320, DOI:10.1016/j.compositesb.2012.04.012

[2] Y. Shi, T. Kashiwagi, R. N. Walters, J. W. Gilman, R. E. Lyon, D. Y. Sogah, Ethylene vinyl acetate/layered silicate nanocomposites prepared by a surfactant-free method: Enhanced flame retardant and mechanical properties, Polymer **50** (2009) 3478 -3487, DOI: 10.1016/j.polymer.2009.06.013

[3] K. Wang, L. Chen, J. Wu, M. L. Toh, C. He, A. F. Yee, Epoxy Nanocomposites with Highly Exfoliated Clay: Mechanical Properties and Fracture Mechanisms, Macromolecules, **38:3** (2005) 788–800, DOI: 10.1021/ma048465n

[4] T.H. Ho and C. S. Wang, Modification of epoxy resins with polysiloxane thermoplastic polyurethane for electronic encapsulation: 1, Polymer **37** (1996) 2733- 2742. DOI: 10.1016/0032-3861(96)87635-X

[5] M. R. Bagherzadeh and F. Mahdavi, Preparation of epoxy–clay nanocomposite and investigation on its anti-corrosive behavior in epoxy coating, Prog. Org. Coat. **60** (2007) 117-120, DOI: 10.1016/j.porgcoat.2007.07.011

[6] Y. Ye, H. Chen, J. Wu, C. M. Chan, Evaluation on the thermal and mechanical properties of HNT-toughened
epoxy/carbon fibre composites
, Composites: Part B **42** (2011) 2145–2150, DOI:10.1016/j.compositesb.2011.05.010

[7] S. Shiu, J. Tsai, Characterizing thermal and mechanical properties of graphene/epoxy nanocomposites
, Composites: Part B **56** (2014) 691–697, DOI: 10.1016/j.compositesb.2013.09.007

[8] H. Gu, S. Tadakamalla, Y. Huang, H. A. Colorado, Z. Luo, N. Haldolaarachchige, D. P. Young, S. Wei, Z. Guo, Polyaniline Stabilized Magnetite Nanoparticle Reinforced Epoxy Nanocomposites, ACS Appl. Mater. Interfaces, **4:10** (2012) 5613–5624, DOI: 10.1021/am301529t

[9] H. Gu, S. Tadakamalla, Xi Zhang, Y. Huang, Y. Jiang, H. A. Colorado, Z. Luo, S. Wei, Z. Guo, Epoxy resin nanosuspensions and reinforced nanocomposites from polyaniline stabilized multi-walled carbon nanotubes, J. Mater. Chem. C**, 1** (2013) 729-743, DOI: 10.1039/C2TC00379A

[10] I. Paulowicz , V. Hrkac , S. Kaps , V. Cretu , O. Lupan , T. Braniste, *et al.* Three-Dimensional SnO_2 Nanowire Networks for Multifunctional Applications: From High-Temperature Stretchable Ceramics to Ultraresponsive Sensors, Adv. Electron. Mater. **1 (**2015) 1500081-89, DOI: 10.1002/aelm.201500081

[11] X. Jin , J. Strueben , L. Heepe , A. Kovalev , *et al.* Joining the Un-Joinable: Adhesion Between Low Surface Energy Polymers Using Tetrapodal ZnO Linkers , Adv. Mater. **24** (2012) 5676–5680, DOI: 10.1002/adma.201201780.

[12] M. Paligova, J. Vilčáková, P. Sáha, V. Křesálek, J. Stejskal, O. Quadrat, Electromagnetic shielding of epoxy resin composites containing carbon fibers coated with polyaniline base, Physica A **335** (2004) 421-429, DOI: 10.1016/j.physa.2003.12.002

[13] H. Chiu, T. Chiang, L. Chen, C. Chang, M. Kuo, Y. Wang, R. Lee, Characteristics, Nano-Dispersibility and Application of Conducting Polypyrrole Inserted into Nitrile Rubber by Single-Step in situ Polymerization, Polym.-Plast. Technol. Eng. **50** (2011) 873-881 DOI**:**10.1080/03602559.2010.551440

[14] B. G. Soares, M. L. Celestino, M. Magioli, V. X. Moreira, D. Khastgir, Synthesis of conductive adhesives based on epoxy resin and polyaniline/DBSA using the in situ polymerization and physical mixing procedures, Synth. Met. 160 (2010) 1981-1986 DOI: 10.1016/j.synthmet.2010.07.021

[15] A. Pud, N. Ogurtsov, A. Korzhenko, G. Shapoval, Some aspects of preparation methods and properties of polyaniline blends and composites with organic polymers, Prog. Polym. Sci. **28** (2003) 1701-1753, DOI: 10.1016/j.progpolymsci.2003.08.001

[16] C. Bao, Y. Guo, L. Song, Y. Kan, X. Qian, Y. Hu, In situ preparation of functionalized graphene oxide/epoxy nanocomposites with effective reinforcements, J. Mater. Chem.**, 21** (2011) 13290-13298, DOI: 10.1039/C1JM11434

[17] A.Pron, P. Rannou, Processible conjugated polymers: from organic semiconductors to organic metals and superconductors, Prog. Polym. Sci. **27** (2002) 135-190, DOI: 10.1016/S0079-6700(01)00043-0

[18] H. Gu, J. Guo, Q. He, S. Tadakamalla, X. Zhang, X. Yan, Y. Huang, H. A. Colorado, S. Wei, Z. Guo, Flame-Retardant Epoxy Resin Nanocomposites Reinforced with Polyaniline-Stabilized Silica Nanoparticles, Ind. Eng. Chem. Res. **52** (2013) 7718−7728, DOI: dx.doi.org/10.1021/ie400275n

[19] Punit Kumar Dhawan, Sanjay Upadhyay, S.K. Verma, Meher Wan, R.R. Yadav, B. Joshi, Size and temperature dependent ultrasonic properties of thermoelectric nanowires, Materials Letters **114** (2014) 15–18, DOI: 10.1016/j.matlet.2013.09.104

[20] D.K. Pandey, P.K. Yadawa, R.R. Yadav, Acoustic wave propagation in Laves-phase compounds, Materials Letters 61:25 (2007) 4747–4751, DOI:10.1016/j.matlet.2007.03.031

[21] M. Wan, R.R. Yadav, K.L. Yadav and S.B. Yadaw, Synthesis and experimental investigation on thermal conductivity of nanofluids containing functionalized Polyaniline nanofibers, Experimental Thermal and Fluid Science **41** (2012) 158-164, DOI: 10.1016/j.expthermflusci.2012.03.030

[22] V. Rajendran, B. Raj, P. Palanichamy, Science and Technology of Ultrasonics, Narosa Publication, New Delhi, 2004. **ISBN:** 978-81-7319-202-9

[23] L. Tang, H. Zhang, J. Han, X. Wu, Z. Zhang, Fracture mechanisms of epoxy filled with ozone functionalized multi-wall carbon nanotubes, Compos.Sci. Technol. **72** (2011) 7-13, DOI: 10.1016/j.compscitech.2011.07.016

[24] K. Sakthipandi, V. Rajendran, On-line phase transitions of bulk and nanocrystalline $La_{1-x}PbxMnO_3$(x = 0.3, 0.4, and 0.5) perovskite manganite materials using ultrasonic measurements, Materials Chemistry and Physics **138** (2013) 581-592, DOI: 10.1016/j.matchemphys.2012.12.023

[25] S. R. White, P. T. Mather, Andm. J. Smith, Characterization of the cure-state of DGEBA-DDS epoxy using ultrasonic, dynamic mechanical and thermal probes, Polymer Engineering and Science **42** (2002) 51-67, DOI: 10.1002/pen.10927

[26] S. Biwa, Y. Watanabe, S. Motogi, N. ohno, Analysis of ultrasonic attenuation in particle-reinforced plastics by a differential scheme, Ultrasonics **43** (2004) 5-12, DOI: 10.1016/j.ultras.2004.03.002

[27] S. Hunklinger, Phonons in Amorphous Materials, Journal De Physique C9: 43 (1982) 461-474, DOI: 10.1051/jphyscol:1982991

[28] A.S. Barker, A. J. Sievers, Optical studies of the vibrational properties of disordered solids, Rev. Mod. Phys. 47 (1975) S1, DOI: 10.1103/RevModPhys.47.S1.2

[29] Zh. Han, A. Fina, Thermal conductivity of carbon nanotubes and their polymer nanocomposites: A review, Prog. Polym. Sci. **36** (2011) 914-944, DOI: 10.1016/j.progpolymsci.2010.11.004

[30] D. E. Kline, Thermal conductivity studies of polymers, J. Polym. Sci. **50** (1961) 441-450, DOI: 10.1002/pol.1961.1205015413

[31] David G. Cahill, R. O. Pohl, Thermal conductivity of amorphous solids above the plateau, Physical Review B **35:8** (1987) 4067-4073, DOI: 10.1103/PhysRevB.35.4067

[32] Robert O. Pohl, Xiao Liu and Eun Joo, Low-temperature thermal conductivity and acoustic attenuation in amorphous solids, Reviews of Modern Physics **74**, 991-1013 (2002), DOI: 10.1103/RevModPhys.74.991

[33] W. Lin, R. Zhang, C. P. Wong, Modeling of Thermal Conductivity of Graphite Nanosheet Composites, Journal of Electronic Materials **39** (2010) 268-272, DOI: 10.1007/s11664-009-1062-2

[34] C. W. Nan, G. Liu, Y. H. Lin, M. Li, Interface effect on thermal conductivity of carbon nanotube composites, Applied Physics Letters **85** (2004) 3549-3551, DOI: 10.1063/1.1808874

[35] T.C. Clancy and T. S. Gates, Modeling of interfacial modification effects on thermal conductivity of carbon nanotube composites, Polymer 47 (2006) 5990-5996, DOI: 10.1016/j.polymer.2006.05.062

[36] M. B. Bryning, D. E. Milkie, M. F. Islam, J. M. Kikkawa, A. G. Yodh, Thermal conductivity and interfacial resistance in single-wall carbon nanotube epoxy composites, Applied Physics Letters 87, 161909 (2005), DOI: 10.1063/1.2103398

[37] A.Balakrishnan, M. C. Saha, Tensile fracture and thermal conductivity characterization of toughened epoxy/CNT nanocomposites, Materials Science and Engineering A 528 (2011) 906-913, DOI: 10.1016/j.msea.2010.09.064

[38] M. J. Assael, K. D. Antoniadis and D. Tzetzis, The use of the transient hot-wire technique for measurement of the thermal conductivity of an epoxy-resin reinforced with glass fibres and/or carbon multi-walled nanotubes, Composites Science and Technology 68 (2008) 3178-3183, DOI: 10.1016/j.compscitech.2008.07.019

[39] W. P. Mason, Physical Acoustics IIIB, (Academic Press Inc., New York, 1965), p. 237.

ACCEPTED MANUSCRIPT

Figures and captions

Fig. 1. SEM images; Fig. 1(a) Pure epoxy, Fig 1(b) Polyaniline nanofibers, Fig. 1(c & d) 1 and 2 wt% Polyaniline nanofibers reinforced Epoxy nanocomposites respectively.

Fig. 2. FTIR spectra of PANI and PANI-Epoxy composites.

Fig. 3. Temperature dependent ultrasonic velocity in Polyaniline nanofibers reinforced epoxy nanocomposites at different fiber loadings.

Fig. 4. Temperature dependent Longitudinal Modulus in Polyaniline nanofibers reinforced epoxy nanocomposites at different fibre loadings.

Fig. 5. Temperature dependent ultrasonic attenuation in Polyaniline nanofibers reinforced epoxy nanocomposites at different fibre loadings.

Fig. 6. Temperature dependent thermal Conductivity in Polyaniline nanofibers reinforced epoxy nanocomposites at different fibre loadings.

Figure. 1

ACCEPTED MANUSCRIPT

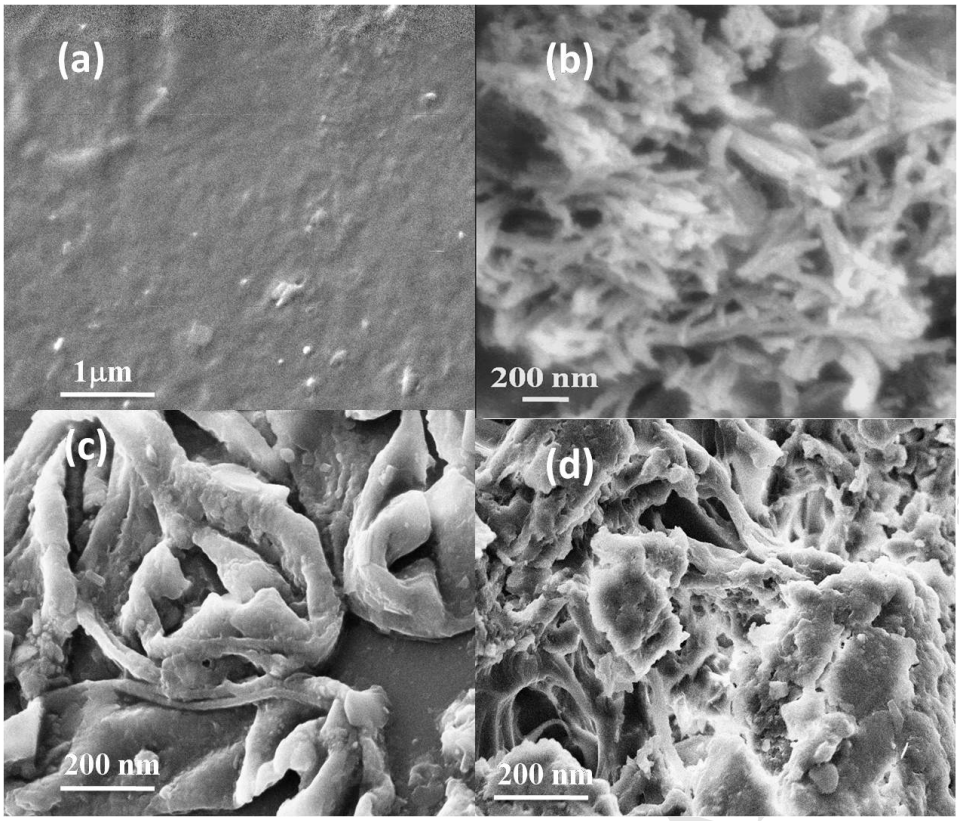

ACCEPTED MANUSCRIPT

Figure .2

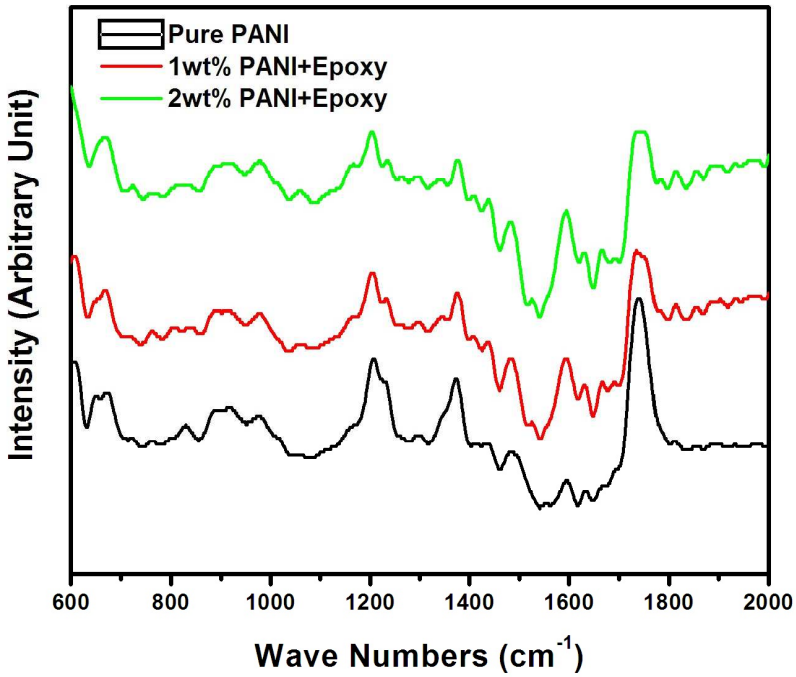

Figure. 3

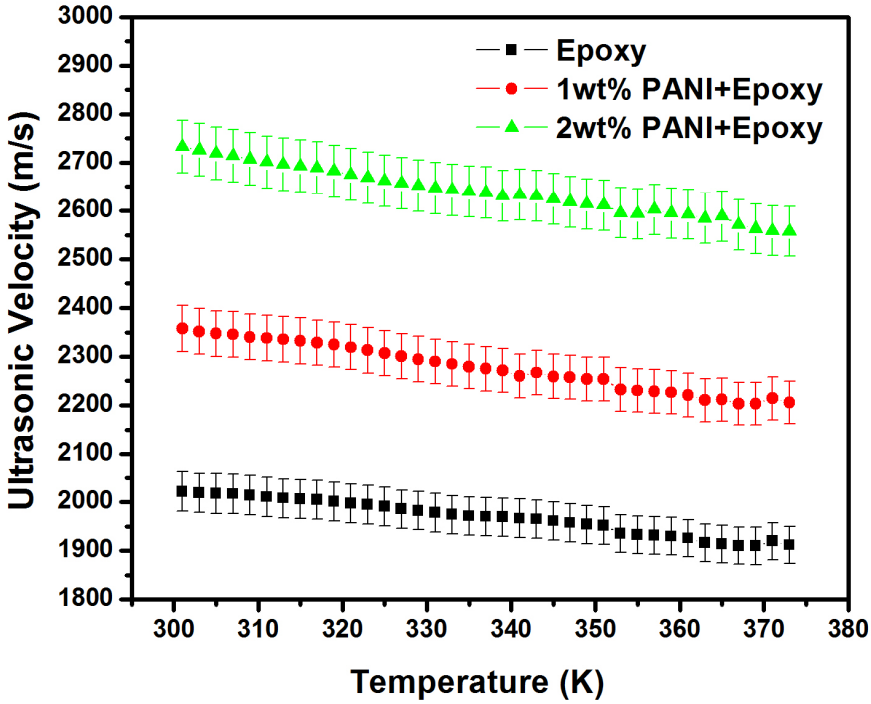
Epoxy
1wt% PANI+Epoxy
2wt% PANI+Epoxy
Ultrasonic Velocity (m/s)
Temperature (K)
3000
2900
2800
2700
2600
2500
2400
2300
2200
2100
2000
1900
1800
300
310
320
330
340
350
360
370
380

Figure. 4

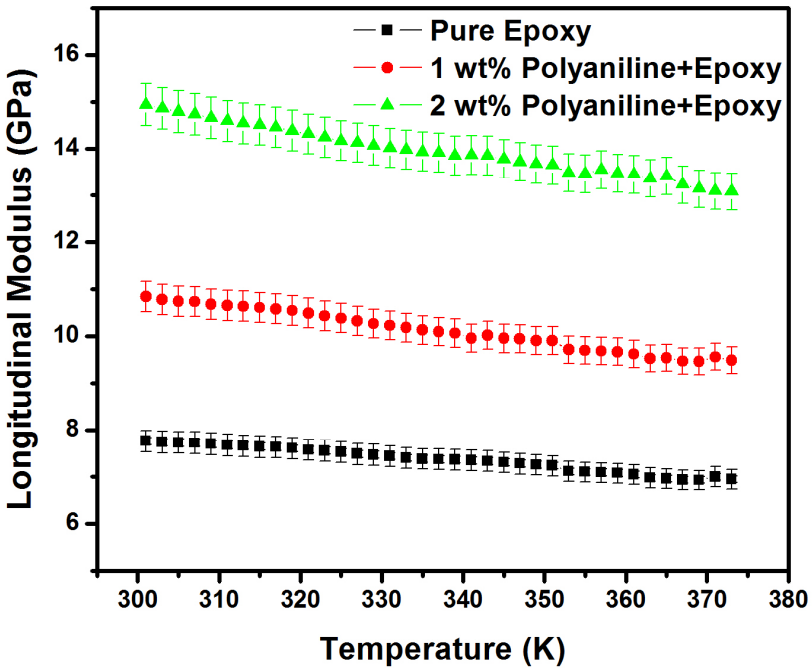

ACCEPTED MANUSCRIPT

Figure. 5

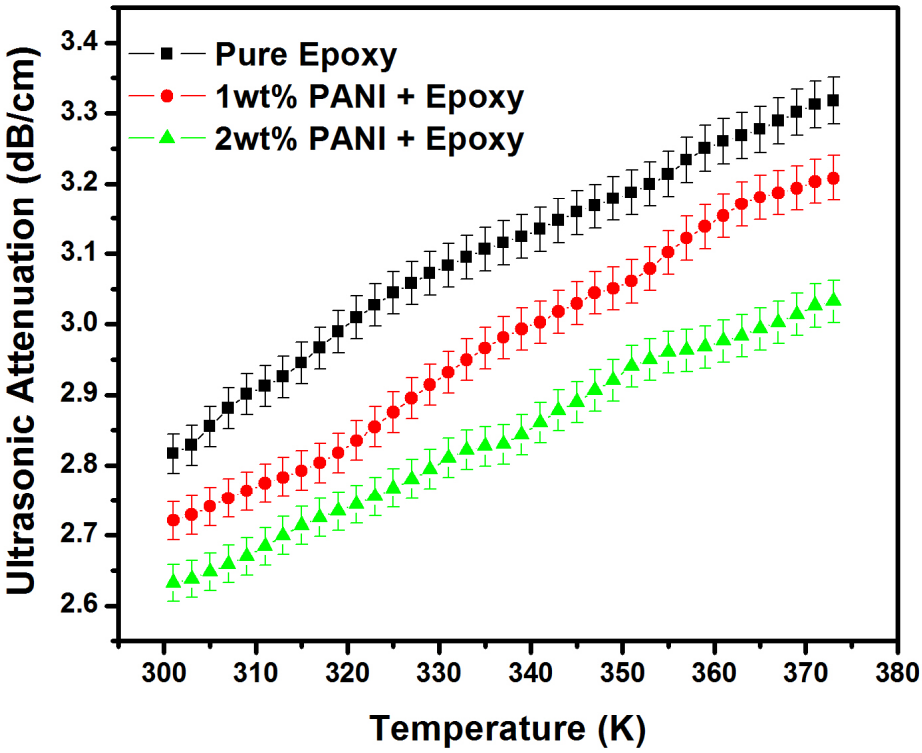

ACCEPTED MANUSCRIPT

Figure. 6

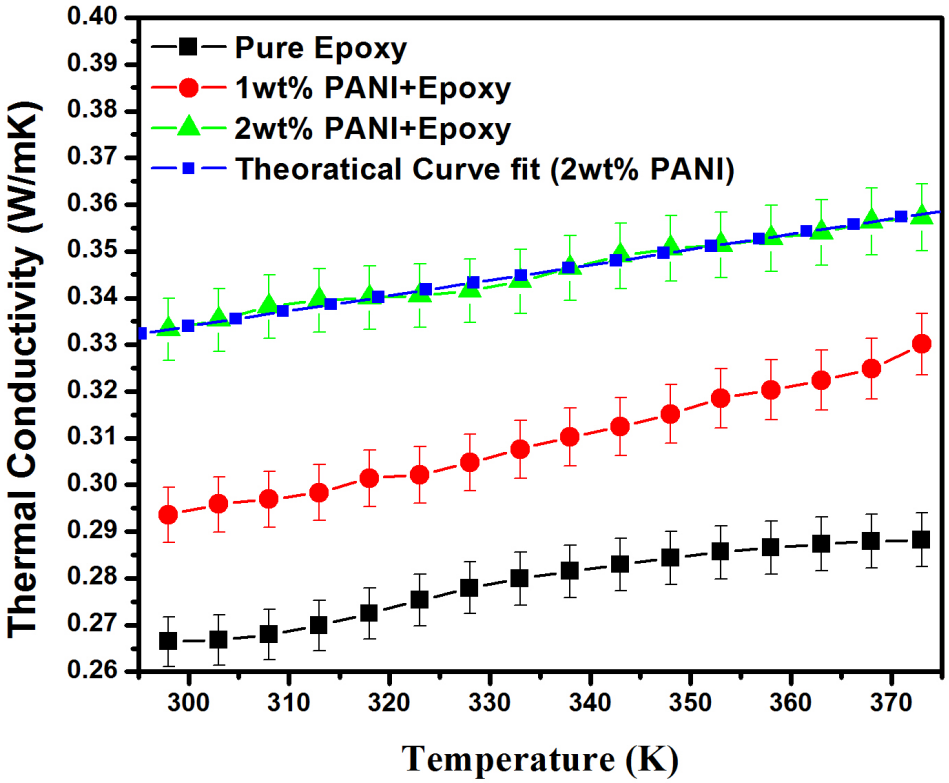

ACCEPTED MANUSCRIPT